Applied Physics Letters

RESEARCH ARTICLE | MAY 30 2023

Thermal conductivity of high-temperature high-pressure synthesized *θ*-TaN

Yizhe Liu ; Qinshu Li ; Yijun Qian ; Yumeng Yang ; Shanmin Wang ; Wu Li ; Bo Sun

Appl. Phys. Lett. 122, 222201 (2023)
https://doi.org/10.1063/5.0146492

AIP Publishing

Applied Physics Letters ARTICLE pubs.aip.org/aip/apl

Thermal conductivity of high-temperature high-pressure synthesized θ-TaN

Cite as: Appl. Phys. Lett. **122**, 222201 (2023); doi: 10.1063/5.0146492
Submitted: 14 February 2023 · Accepted: 9 May 2023 ·
Published Online: 30 May 2023

Yizhe Liu,[1] Qinshu Li,[1] Yijun Qian,[2] Yumeng Yang,[2] Shanmin Wang,[3] Wu Li,[4] and Bo Sun[1,5,a)]

AFFILIATIONS

[1]Tsinghua-Berkeley Shenzhen Institute, Tsinghua University, Shenzhen 518055, China
[2]School of Information Science and Technology, ShanghaiTech University, Shanghai 201210, China
[3]Department of Physics, Southern University of Science and Technology, Shenzhen 518055, China
[4]Institute for Advanced Study, Shenzhen University, Shenzhen 518060, China
[5]Tsinghua Shenzhen International Graduate School and Guangdong Provincial Key Laboratory of Thermal Management Engineering & Materials, Shenzhen 518055, China

[a)]Author to whom correspondence should be addressed: sun.bo@sz.tsinghua.edu.cn

ABSTRACT

Recent first-principles calculation predicted that theta phase tantalum nitride (θ-TaN) single crystal has an ultrahigh thermal conductivity of $\sim$1000 W m^{-1} K^{-1} at room temperature, making it one of the best thermal conductors among all materials. Here, we have synthesized θ-TaN by phase change from ε-TaN powder at 1750 K and 7.8 GPa. X-ray diffraction patterns and scanning transmission electron microscopy indicate that the as-prepared θ-TaN has a hexagonal tungsten carbide structure with an average grain size of 45 nm. The room-temperature thermal conductivity of θ-TaN was measured to be 47.5 W m^{-1} K^{-1} using time-domain thermoreflectance. Temperature-dependent thermal conductivity suggests that phonon-boundary scattering dominates thermal transport. The thermal conductivity of our sample is higher than those of Si and SiC nanostructures with the same characteristic length. Our result suggests that it is probable to further increase the thermal conductivity of θ-TaN.

Thermal management of microelectronic devices has received extensive attention with increasing power densities.[1–3] Efficient heat dissipation requires thermally conductive materials and interfaces.[4–7] While diamond and boron arsenide (BAs) are believed to be the best thermal conductors so far where phonon dominates heat conduction, metals have limited thermal conductivity as the electron–phonon scattering reduces their conductivities. For example, silver has the largest thermal conductivity of 427 W m^{-1} K^{-1} in all metals, which is much smaller than those of diamond and BAs.[8] In 2021, a first-principles calculation proposed that the triply degenerate topological semimetal theta phase tantalum nitride (θ-TaN) (space group: P$\bar{6}$m2, No. 187) has an ultrahigh thermal conductivity of 995 and 820 W m^{-1} K^{-1} along a and c axes at room temperature, whose thermal conductivity exceeds those of all known metals.[9] In θ-TaN, phonons are found to dominate thermal transport and the ultrahigh thermal conductivity is attributed to the weak electron-phonon scattering as well as the large frequency gap between acoustic and optical phonon modes. The frequency gap impedes three-phonon processes while increases channels for higher-order phonon scattering, making θ-TaN a potential candidate to study the four-phonon process.[9] Compared with other metallic materials, such as graphite, θ-TaN shows no significant anisotropy. The hexagonal tungsten carbide (WC) structure of θ-TaN provides it a Vickers hardness of 26 GPa due to strong covalent bonds.[10] Hence, θ-TaN is promising for heat dissipation in electronic industries and many other applications.

Although the binary phase diagram of TaN has been constructed several years ago,[11] the requirement of high pressure and temperature (above 3 GPa and 800 K) makes growing θ-TaN a challenging task. The volume change during phase transition significantly reduces the stability of the synthesis process. Due to the difficulties in crystal growth, the experimental results of θ-TaN are still lacking. Recently, Lee *et al.*[12] presented the synthesis of polycrystalline θ-TaN under high temperatures (1500–2000 K) and high pressure (4.2 GPa). The thermal conductivities of their samples at room temperature vary from 15.7 to 90.3 W m^{-1} K^{-1}, showing an obvious inconsistency in sample quality. The x-ray diffraction (XRD) patterns also show impurity peaks corresponding with the precursor, which indicates the phase transition was not complete. In this Letter, we reported the synthesis and

characterization of bulk θ-TaN polycrystals. The θ-TaN polycrystals were prepared under high temperature and high pressure by phase transition from ε-TaN, which is stabilized employing a three-stage heating process. XRD patterns showed no impurity peaks and the polycrystalline grain size of 45 nm. The thermal conductivity (Λ) and electrical resistivity (ρ) were measured to be 47.5 W m^{-1} K^{-1} and 2.4 $\mu\Omega$ m at room temperature. To estimate the Λ of bulk θ-TaN single crystal, we compared Λ of our sample with those of Si and silicon carbide (SiC) nanostructures with the same characteristic length. The comparison suggests a possibly higher Λ of single crystal θ-TaN than those of Si and SiC. Our results show the potential of θ-TaN as a thermal conductor, and further development of growing single crystals is needed.

Before the synthesis of θ-TaN, the precursor ε-TaN powder (Alfa Aesar, 99.5%, 325 mesh) was compacted into a small pellet with 8.3 mm in diameter and 2 mm in height. The tightly compressed ε-TaN powder prevents volume collapse during phase transition. The pellet was loaded into a Ta capsule, which was then placed into a NaCl tube. The surrounded NaCl was used for pressure transfer and thermal insulation. Next, we embedded the cell into a graphite tube and sealed it with two steel sheets, which electrically connect with top and bottom WC anvils and serve as the heater through Joule heating. A dehydrated pyrophyllite cube was employed as the container to thermally insulate the graphite tube. High-temperature high-pressure synthesis experiment was carried out in a DS 6 × 10 MN cubic press and square faceted WC anvils were employed to triaxially exert force on the pyrophyllite container, generating high pressure inside the cell.[13] The pressure is required to increase uniformly and slowly to maintain a stable pressure. We achieved the target pressure of 7.8 GPa within 2 h and then kept it for 0.5 h to guarantee homogenous pressure distribution. We took the most concern on the heating procedure as a small fluctuation in temperature can lead to abrupt pressure change and fail the experiment, especially around the phase transition point. Hence, we divided the heating process into three stages. The first stage was below 500 K, where the temperature was not high and the heating rate was set to be 50 K/min to increase the temperature quickly. The second stage was 500–800 K, which was approaching the phase transition point and the heating rate was reduced to 30 K/min. When the temperature exceeded 800 K, the heating rate was limited to 10 K/min until 1750 K to stabilize the phase transition process. The temperature was maintained for 0.5 h. The selection of pressure, temperature, and heating rate was a trade-off between the growth difficulties and crystal grain size. Then, the system was cooled down at a rate of 50 K/min, followed by pressure relief in 1 h. The aggregated grains were cleaned using nitric acid to remove excess Ta and washed with de-ionized water and ethanol to obtain pure samples for further characterization and measurements.

XRD measurement was performed to determine the structure and crystallinity of the obtained samples. We crushed the as-prepared bulk sample into powder for XRD measurement. Figure 1 shows that the XRD pattern has nine diffraction peaks at 31.1°, 35.4°, 47.8°, 63.5°, 64.7°, 72.4°, 74.8°, 76.0°, and 83.2°, corresponding to (001), (100), (101), (110), (002), (111), (200), (102), and (201) lattice planes of θ-TaN (ICDD: 04–004-6839), respectively. No apparent impurity peak was observed, confirming the high purity of our sample. Noting that the sample has quite broad diffraction peaks, implying the small grain size. To estimate the grain size L, we applied the Scherrer equation as follows:

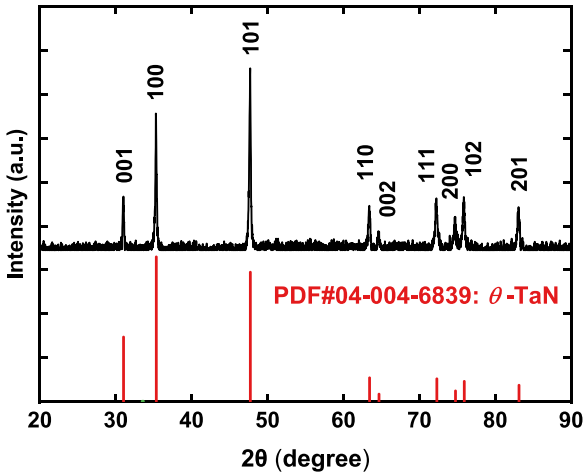

FIG. 1. The XRD patterns of θ-TaN powder.

$$L = K\lambda/\beta\cos\theta, \tag{1}$$

where K is a dimensionless shape factor with a typical value of 0.94, λ of 0.1542 nm is the average x-ray wavelength emitted from a copper target, θ is the Bragg angle, and β is the FWHM of the selected peak.[14] A typical peak at 47.8° was chosen, whose FWHM is 0.21° by fitting the curve with a Lorentzian function. As a result, the grain size was calculated to be 45 nm. We further characterized the sample employing scanning transmission electron microscopy (STEM). We selected a representative region and the periodic hexagonal structure was shown in Fig. 2(a), where expected spacings of 0.254 nm and 0.191 nm were consistent with the (010) and (101) lattice planes, respectively. The selected area electron diffraction (SAED) was later conducted in the region and Fig. 2(b) exhibits typical single crystal patterns along the [$\bar{1}0\bar{1}$] zone axis, which is inspiring for pursuing bulk θ-TaN single crystals with high crystallinity.

We measured the thermal conductivity Λ using time-domain thermoreflectance (TDTR), which is a non-contact pump-probe technique to extract thermal properties of a wide range of materials.[15–17] Briefly, we split the pulsed femtosecond laser (785 nm, 80 MHz repetition rate) into two beams by a polarizing beam splitter. The pump laser beam is modulated at a radio frequency of 0.21 MHz by an electro-optical modulator to heat the sample and generate periodic temperature oscillations on the sample surface. The low frequency is used to avoid thermal nonequilibrium that affects TDTR measurements.[18,19] The probe beam, modulated at an audio frequency of 200 Hz by a mechanical chopper, monitors the temperature-dependent reflectance change from the surface. Before the measurement, we polished the sample and deposited an Al film of 80 nm on the sample surface via electron beam evaporation, serving as the thermoreflectance transducer. The signal with respect to the delay time between pump and probe beams was demodulated through lock-in amplifiers, which was later fitted using a diffusive thermal model to extract thermal properties.[15] Figure 3(a) illustrates the typical TDTR data, from which a Λ of 47.5 W m^{-1} K^{-1} is obtained at room temperature. The measured Λ is only ~1/20 of the predicted value from first-principles,[9] indicating strong phonon scattering by grain boundaries. We then conducted the measurement from 80 to 500 K and made comparisons with phonon thermal conductivities (Λ_{ph}) calculated

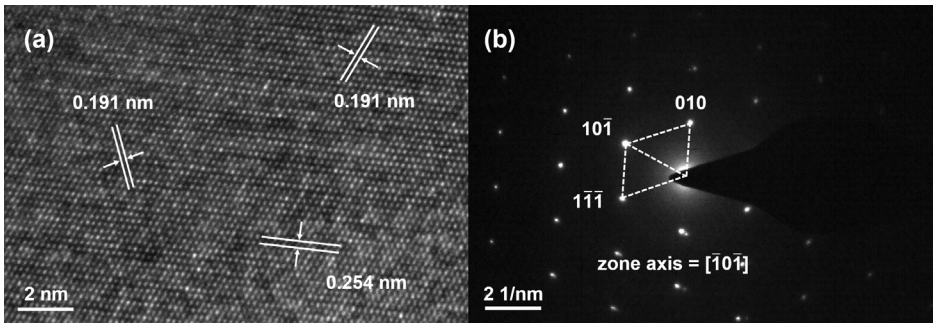

FIG. 2. (a) STEM image of θ-TaN in the selected region. (b) SAED patterns along $[\bar{1}0\bar{1}]$ zone axis.

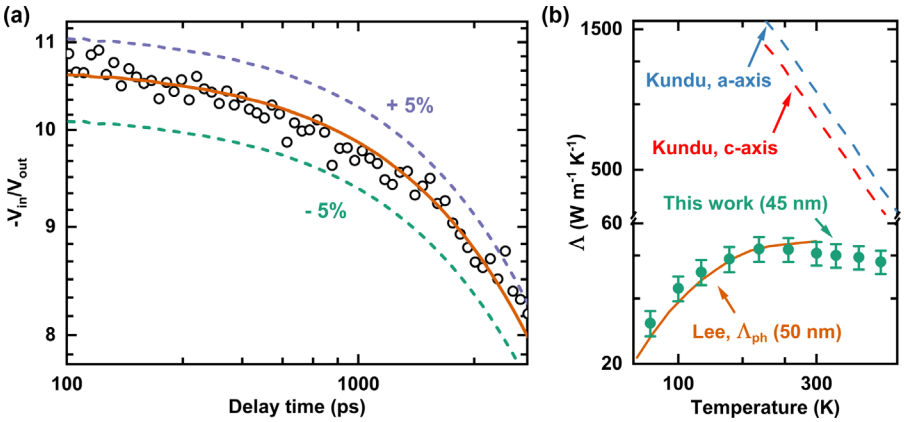

FIG. 3. (a) TDTR data of θ-TaN at room temperature. We fit the experimental data (black circles) using a diffusive multilayer thermal model to obtain the Λ (orange solid line). Plots with the Λ changed by +5% (purple dashed line) and −5% (green dashed line) of the best values illustrate the fitting uncertainty. (b) Temperature-dependent thermal conductivities of θ-TaN. The green circles represent the experimental values of this work while the orange solid line shows the calculated Λ_{ph} by Lee *et al.*[12] with a grain size of 50 nm. The dashed lines represent predicted bulk values by Kundu *et al.*[9] along the a axis (blue) and c axis (red), respectively.

by first-principles at a similar grain size (50 nm), as shown in Fig. 3(b).[12] The measured temperature-dependent thermal conductivities agree well with the calculation, which shows a typical trend dominated by phonon-boundary scattering.

To further evaluate the quality of θ-TaN polycrystals, we conducted electrical measurement using the Van der Pauw method, and a ρ value of 2.4 $\mu\Omega$ m is extracted with an uncertainty of 5% at room temperature.[20] Based on the Wiedemann–Franz law,[21] the thermal conductivity contributed by electrons was estimated to be 3.3 W m^{-1} K^{-1} and the lattice thermal conductivity Λ_{ph} can be calculated as 44.2 W m^{-1} K^{-1}, corresponding to the first-principles prediction that phonons are main heat carriers in θ-TaN. For comparison, Λ of TaN reported by Lee *et al.*[12] ranges from 15.7 to 90.3 W m^{-1} K^{-1}, while ρ varies from 1.9 to 5.4 $\mu\Omega$ m with grain size from 33.8 to 62.5 nm.

Since the grain boundary strongly scatters heat-carrying phonons and suppresses the Λ of our sample, we compare Λ of our sample with those of Si and SiC nanostructures, as shown in Fig. 4. The Λ of our θ-TaN is about twice larger than those of Si nanowires[22,23] with similar characteristic lengths and is higher than those of Si and SiC thin films.[24–26] The comparison indicates that bulk θ-TaN might have a Λ higher than that of Si or SiC, though such comparison is rather rough as they have different phonon mean free path distributions. Since materials with high Λ normally have long phonon mean free paths, larger crystals of θ-TaN are needed for a decisive conclusion on its thermal conductivity.

In summary, high purity θ-TaN polycrystals with a grain size of 45 nm were synthesized using the high-temperature high-pressure

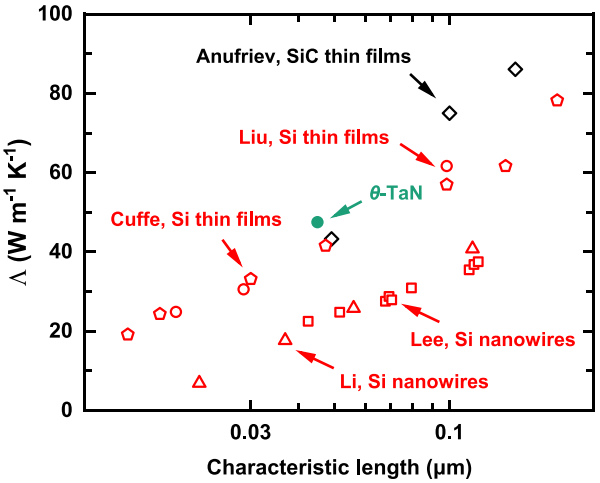

FIG. 4. Thermal conductivities of θ-TaN (green circle), Si (red), and SiC (black). The red triangles by Li *et al.*,[22] red squares by Lee *et al.*,[23] red pentagons by Cuffe *et al.*,[25] and red circles by Liu *et al.*[24] represent the measured thermal conductivities of Si nanostructures. The black diamonds by Anufriev *et al.*[26] show the measured thermal conductivities of SiC thin films.

method at 1750 K and 7.8 GPa. Detailed synthesis steps were reported to stabilize the phase transition process. XRD patterns show the sample has a hexagonal WC structure, which is consistent with our STEM results. The room-temperature Λ of 47.5 W m^{-1} K^{-1} and ρ of 2.4 $\mu\Omega$ m

are in the range of the recent publication of Lee *et al.*[12] Temperature-dependent TDTR measurements agree well with first-principles calculation, indicating that phonon boundary scattering dominates thermal transport. The measured Λ of our polycrystalline θ-TaN is higher than those of Si and SiC nanostructures with the same characteristic length, which suggests a possible higher Λ for single crystals. Our results show that θ-TaN probably has a high Λ, which advances the search for high thermal conductivity materials.

We acknowledge the funding support from the National Natural Science Foundation of China (Nos. 12004211 and 52161145502), the Shenzhen Science and Technology Program (Nos. RCYX20200714114643187 and WDZC20200821100123001), and the Tsinghua Shenzhen International Graduate School (Nos. QD2021008N and JC2021008).

AUTHOR DECLARATIONS

Conflict of Interest

The authors have no conflicts to disclose.

Author Contributions

Yizhe Liu: Data curation (lead); Formal analysis (lead); Investigation (lead); Methodology (lead); Validation (lead); Writing – original draft (lead). **Qinshu Li:** Data curation (supporting). **Yijun Qian:** Data curation (supporting). **Yumeng Yang:** Supervision (supporting). **Shanmin Wang:** Supervision (supporting). **Wu Li:** Supervision (supporting). **Bo Sun:** Funding acquisition (equal); Project administration (equal); Supervision (equal); Writing – review & editing (equal).

DATA AVAILABILITY

The data that support the findings of this study are available from the corresponding author upon reasonable request.

REFERENCES

[1]P. Ball, Nature **492**, 174 (2012).
[2]M. M. Waldrop, Nature **530**, 144 (2016).
[3]B. Sun, G. Haunschild, C. Polanco, J. Ju, L. Lindsay, G. Koblmüller, and Y. K. Koh, Nat. Mater. **18**, 136 (2019).
[4]Q. Li, F. Liu, S. Hu, H. Song, S. Yang, H. Jiang, T. Wang, Y. K. Koh, C. Zhao, F. Kang, J. Wu, X. Gu, B. Sun, and X. Wang, Nat. Commun. **13**, 4901 (2022).
[5]J. S. Kang, M. Li, H. Wu, H. Nguyen, and Y. Hu, Science **361**, 575 (2018).
[6]S. Li, Q. Zheng, Y. Lv, X. Liu, X. Wang, P. Y. Huang, D. G. Cahill, and B. Lv, Science **361**, 579 (2018).
[7]F. Tian, B. Song, X. Chen, N. K. Ravichandran, Y. Lv, K. Chen, S. Sullivan, J. Kim, Y. Zhou, T.-H. Liu, M. Goni, Z. Ding, J. Sun, G. A. G. Udalamatta Gamage, H. Sun, H. Ziyaee, S. Huyan, L. Deng, J. Zhou, A. J. Schmidt, S. Chen, C.-W. Chu, P. Y. Huang, D. Broido, L. Shi, G. Chen, and Z. Ren, Science **361**, 582 (2018).
[8]R. Powell, C. Y. Ho, and P. E. Liley, *Thermal Conductivity of Selected Materials* (U.S. Department of Commerce, National Bureau of Standards Washington, DC, 1966), p. 51.
[9]A. Kundu, X. Yang, J. Ma, T. Feng, J. Carrete, X. Ruan, G. K. H. Madsen, and W. Li, Phys. Rev. Lett. **126**, 115901 (2021).
[10]L.-H. Feng, Q.-W. Hu, L. Lei, L.-M. Fang, L. Qi, L.-L. Zhang, M.-F. Pu, Z.-L. Kou, F. Peng, X.-P. Chen, Y.-H. Xia, Y. Kojima, H. Ohfuji, D.-W. He, B. Chen, and T. Irifune, Chin. Phys. B **27**, 026201 (2018).
[11]A. Friedrich, W. Morgenroth, L. Bayarjargal, E. A. Juarez-Arellano, B. Winkler, and Z. Konôpková, High Pressure Res. **33**, 633 (2013).
[12]H. Lee, Y. Zhou, S. Jung, H. Li, Z. Cheng, J. He, J. Chen, P. Sokalski, A. Dolocan, R. Gearba-Dolocan, K. C. Matthews, F. Giustino, J. Zhou, and L. Shi, Adv. Funct. Mater. **33**, 2212957 (2023).
[13]X. Zhou, D. Ma, L. Wang, Y. Zhao, and S. Wang, Rev. Sci. Instrum. **91**, 015118 (2020).
[14]A. L. Patterson, Phys. Rev. **56**, 978 (1939).
[15]D. G. Cahill, Rev. Sci. Instrum. **75**, 5119 (2004).
[16]A. J. Schmidt, X. Chen, and G. Chen, Rev. Sci. Instrum. **79**, 114902 (2008).
[17]B. Sun and Y. K. Koh, Rev. Sci. Instrum. **87**, 064901 (2016).
[18]Y. K. Koh, D. G. Cahill, and B. Sun, Phys. Rev. B **90**, 205412 (2014).
[19]B. Sun, X. Gu, Q. Zeng, X. Huang, Y. Yan, Z. Liu, R. Yang, and Y. K. Koh, Adv. Mater. **29**, 1603297 (2017).
[20]S. Lim, D. McKenzie, and M. Bilek, Rev. Sci. Instrum. **80**, 075109 (2009).
[21]R. Franz and G. Wiedemann, Ann. Phys. Chem. **165**, 497 (1853).
[22]D. Li, Y. Wu, P. Kim, L. Shi, P. Yang, and A. Majumdar, Appl. Phys. Lett. **83**, 2934 (2003).
[23]J. Lee, W. Lee, J. Lim, Y. Yu, Q. Kong, J. J. Urban, and P. Yang, Nano Lett. **16**, 4133 (2016).
[24]W. Liu and M. Asheghi, J. Heat Transfer **128**, 75 (2006).
[25]J. Cuffe, J. K. Eliason, A. A. Maznev, K. C. Collins, J. A. Johnson, A. Shchepetov, M. Prunnila, J. Ahopelto, C. M. Sotomayor Torres, G. Chen, and K. A. Nelson, Phys. Rev. B **91**, 245423 (2015).
[26]R. Anufriev, Y. Wu, J. Ordonez-Miranda, and M. Nomura, NPG Asia Mater. **14**, 35 (2022).